

ORIGINAL STUDIES

Multicenter clinical evaluation of a piezoresistive-MEMS-sensor rapid-exchange pressure microcatheter system for fractional flow reserve measurement

Chenguang Li MD¹  | Junqing Yang MD² | Shaohong Dong MD³ |
 Liang Dong MD⁴ | Jiyan Chen MD² | Li Shen MD¹ | Feng Zhang MD¹ |
 Changling Li MD⁴ | Huadong Liu MD³ | Xinyang Hu MD⁴ |
 William Kongto Hau PhD⁵ | Juying Qian MD¹ | Allen Jeremias MD, MSc^{6,7} |
 Jian'an Wang MD⁴ | Junbo Ge MD¹  | for the SUPREME Study Investigators

¹Department of Cardiology, Zhongshan Hospital, Fudan University, Shanghai, China

²Department of Cardiology, Guangdong Provincial People's Hospital, Guangzhou, Guangdong, China

³Department of Cardiology, Shenzhen People's Hospital, Shenzhen, Guangdong, China

⁴Department of Cardiology, The Second Affiliated Hospital, Zhejiang University School of Medicine, Zhejiang, Hangzhou, China

⁵Department of Medicine and Therapeutics, Faculty of Medicine, The Chinese University of Hong Kong, Hong Kong, China

⁶Department of Cardiology, St. Francis Hospital, Roslyn, New York, New York

⁷Clinical Trials Center, Cardiovascular Research Foundation, New York, New York

Correspondence

Dr Junbo Ge, Department of Cardiology,
 Zhongshan Hospital, Fudan University,
 180 Fenglin Road, Xu Hui District, Shanghai,
 China 200032.

Email: jbge@zs-hospital.sh.cn

Abstract

Objectives: This multicenter, prospective clinical study investigates whether the microelectromechanical-systems-(MEMS)-sensor pressure microcatheter (MEMS-PMC) is comparable to a conventional pressure wire in fractional flow reserve (FFR) measurement.

Background: As a conventional tool for FFR measurement, pressure wires (PWs) still have some limitations such as suboptimal handling characteristics and unable to maintain the wire position during pullback assessment. Recently, a MEMS-PMC compatible with any 0.014" guidewire is developed. Compared with the existing optical-sensor PMC, this MEMS-PMC has smaller profiles at both the lesion crossing and sensor packaging areas.

Methods: Two hundred and forty-two patients with visually 30–70% coronary stenosis were enrolled at four centers. FFR was measured first with the MEMS-PMC, and then with the PW. The primary endpoint was the Bland–Altman mean bias between the MEMS-PMC and PW FFR.

Results: From the 224-patient per-protocol data, quantitative coronary angiography showed 17.9% and 55.9% vessels had diameter < 2.5 mm and stenosis >50%, respectively. The two systems' mean bias was –0.01 with [–0.08, 0.06] 95% limits-of-agreement. Using PW FFR≤0.80 as cutoff, the MEMS-PMC per-vessel diagnostic accuracy was 93.4% [95% confidence interval: 89.4–96.3%]. The MEMS-PMC's success rate

This is an open access article under the terms of the Creative Commons Attribution-NonCommercial License, which permits use, distribution and reproduction in any medium, provided the original work is properly cited and is not used for commercial purposes.

© 2021 The Authors. *Catheterization and Cardiovascular Interventions* published by Wiley Periodicals LLC.

was similar to that of PW (97.5 vs. 96.3%, $p = .43$) with no serious adverse event, and its clinically-significant (>0.03) drift rate was 43% less (9.5 vs. 16.7%, $p = .014$).

Conclusions: Our study showed the MEMS-PMC is safe to use and has a minimal bias equal to the resolution of current FFR systems. Given the MEMS-PMC's high measurement accuracy and rapid-exchange nature, it may become an attractive new tool facilitating routine coronary physiology assessment.

KEYWORDS

coronary artery disease, catheterization, diagnostic, clinical trials, coronary blood flow/physiology/microvascular function, fractional flow reserve, percutaneous coronary intervention

1 | INTRODUCTION

Over the past decade, the clinical benefits of using fractional flow reserve (FFR) for guiding percutaneous coronary intervention (PCI) have been well demonstrated in several important clinical studies.¹⁻³ Supported by a wealth of long-term clinical data,⁴⁻⁶ FFR is widely recognized as the reference standard for assessing the functional significance of coronary artery stenosis^{7,8} and is widely used in the catheterization laboratory (cathlab) for PCI.⁹ Currently, pressure wires (PWs) are the conventional tool for FFR measurement but suffer from several limitations, including: (a) usually less desirable maneuverability compared with the best-in-class guidewires, owing to the hollow-structured shaft of PWs required for housing electrical wires or optical fibers; (b) potential complication risks for re-wiring the vessels or lesions during pullback and post-intervention FFR assessment^{10,11}; (c) dis- and re-connecting the PWs' signal terminals may be needed, which can increase the drift probability.

An optical-sensor pressure microcatheter (Navvus, ACIST Medical Systems, Eden Prairie, MN, USA) accommodating any 0.014" guidewire has been developed¹² and investigated in several clinical studies.¹³⁻¹⁶ It has been shown that FFR measurement using pressure microcatheter (PMC) facilitates multiple advancement and withdrawal over any guidewire of physicians' choice. In addition, during physiological assessment for diffuse and serial lesions, the PMC enables maintaining the guidewire in place. The optical-sensor pressure microcatheter has been shown to have a mean bias of -0.02 from PW, and a 97% clinical decision concordance with PW when taking the gray zone into account, which is regarded to be of minimal diagnostic impact for most cases.¹⁴

Piezoresistive microelectromechanical system (MEMS) pressure sensors fabricated using semiconductor process can enable smaller overall dimensions and a lower cost compared with optical pressure sensors. Recently, a new type of PMC integrating a piezoresistive MEMS sensor has been recently developed (TruePhysio, Insight Lifetech, Shenzhen, China). Compared with the existing 0.022" optical-sensor PMC, this rapid-exchange MEMS-sensor pressure microcatheter (MEMS-PMC) has: (a) an $\sim 13\%$ reduced cross-section area at the lesion crossing position; (b) a shorter and smaller sensor packaging area; (c) a shorter tip to sensor distance. In principle, such

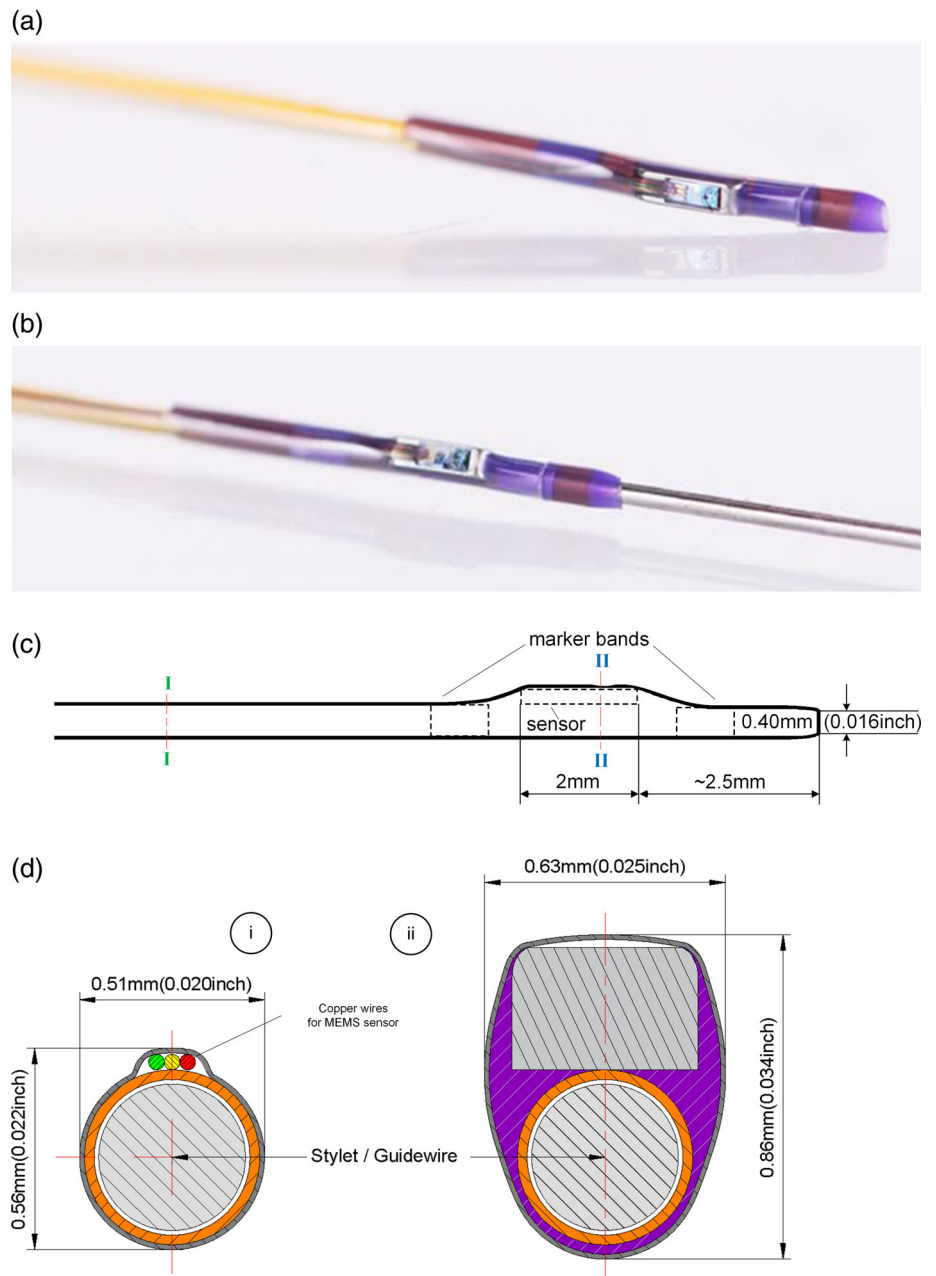
features may lead to an increased measurement agreement (with the PW) and improved crossability than the optical-sensor PMC. However, as the first clinical evaluation of the MEMS-PMC, here we aimed to prospectively evaluate the safety and efficacy of this device. The primary endpoint was the Bland-Altman mean bias between the FFR of MEMS-PMC and PW systems. Secondary endpoints included correlation, diagnostic performance (accuracy, sensitivity, and specificity), receiver operating characteristic (ROC) analysis, and drift evaluation.

2 | METHODS

2.1 | The MEMS-sensor-equipped rapid-exchange PMC system

The MEMS-PMC system consists of a PMC and a console. The rapid-exchange PMC is equipped with a piezoresistive, proprietarily packaged pressure sensor (Figure 1a,b). This sensor is positioned approximately 2.5 mm from the distal entry (Figure 1c), which is $\sim 50\%$ closer compared with the existing optical-sensor PMC.¹² The rapid-exchange segment has a lumen that accommodates any 0.014" guidewire (Figure 1b,c). The cross-section (Figure 1d (i)) of the expected lesion position "I-I" (Figure 1c) has two dimensions: 0.020" and 0.022" (Figure 1d (i)), with an equivalent diameter 0.0205" after circular conversion. Two metallic marker bands are 3 mm apart, one distal and the other proximal (Figure 1c), and they "sandwich" the sensor. Such a dual-band design enables better sensor positioning and estimation of lesion lengths. The piezoresistive sensor is windowed at position "II-II" (cross-section in Figure 1c,d (ii)). Note that, although the sensor position represents the largest profile (0.034" \times 0.025") of the catheter, it does not locate at the lesion crossing, and has a length of less than 2 mm, which is expected to have a minimal impact on the blood flow. The rest of the tip is made of composite polymeric layers for a balanced pushability and flexibility properties with conducting wires embedded (Figure 1d (i)). The console with a touch-screen monitor (VivoCardio, Insight Lifetech, Shenzhen, China) receives the pressure signals and displays the pressure waveforms in real time. The mean aortic and distal pressure values averaged over three heart beats are used to calculate P_d/P_a , and thus FFR under hyperemia.

FIGURE 1 Main features of the MEMS-PMC. (a) The tip segment of MEMS-PMC; (b) MEMS-PMC over a 0.014" stylet; (c) Schematic of the MEMS-PMC tip, where (d)-(i) delineates its cross-section at "I-I" position with the lesion-position dimensions, and (d)-(ii) delineates its cross-section at "II-II". MEMS-PMC, MEMS-sensor equipped pressure microcatheter; PW, pressure wire



2.2 | Patient inclusion criteria and enrollment

This study was conducted with compliance of the Declaration of Helsinki. The institutional review board or ethics committee at each participating center, including Zhongshan Hospital, Guangdong Provincial People's Hospital, Shenzhen People's Hospital, and The Second Affiliated Hospital of Zhejiang University, has reviewed and approved the study protocol. The study followed the controlled flow chart shown in Figure 2a. The eligible patients were between 18 and 75 years of age, with indications for FFR. The target vessels had a single de novo lesion with visual reference vessel diameter (RVD) ≥ 2.5 mm and intermediate severity (visually 30–70% diameter stenosis, DS). Patients with following conditions were excluded from the study: ST-segment elevation myocardial infarction (STEMI), non-ST-segment elevation myocardial

infarction (NSTEMI), left main disease, thrombosis or dissection in target vessel, in-stent restenosis, a left ventricular ejection fraction $<30\%$, severe heart failure (NYHA Class IV, NYHA: New York Heart Association), extremely tortuous or calcified stenosis, chronic total occlusion, contraindication to adenosine-5'-triphosphate (ATP) or PCI. All participants included in the study had signed the written informed consent form (Figure 2a). There was no formal Patient and Public Involvement in the design or conduct of this study.

2.3 | Procedural protocol and implementation

The clinical protocol was established based on the previously known best practice guidelines for FFR measurement^{17,18} and is summarized

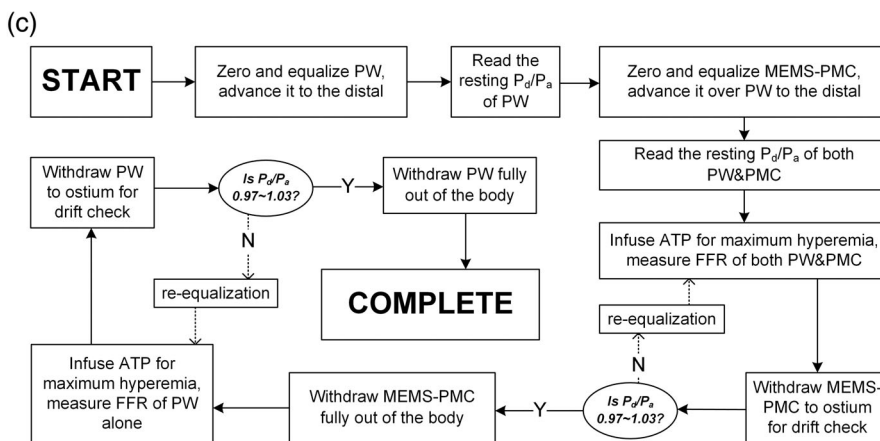
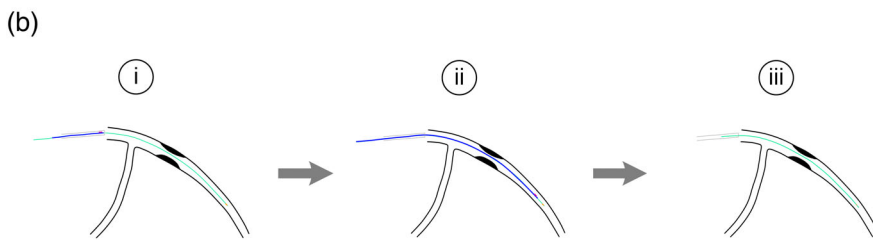
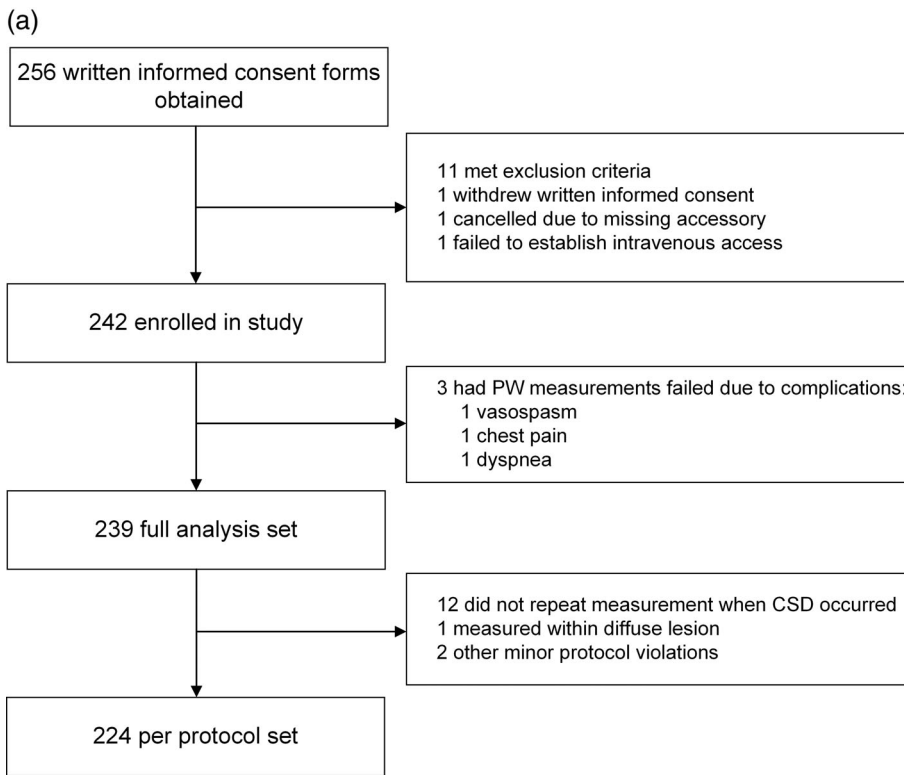


FIGURE 2 Trial enrollment flowchart and stepwise measuring procedure.

(a) Trial enrollment flowchart. The patients with signed informed consent forms were enrolled according to the flowchart. Among the 242 successfully enrolled patients, 3 failed to complete FFR measurement for both MEMS-PMC and PW FFR data. Data coordinating center determines further excluding 15 patients underwent procedure as a result of protocol violations. The valid MEMS-PMC and PW FFR data sets appropriate for analysis are from the rest 224 patients. (b) Illustrated PW and MEMS-PMC FFR measuring procedure: (i) The MEMS-PMC entering the ostium over a PW; (ii) FFR measured with a MEMS-PMC over a PW; (iii) FFR measured with the PW alone. (c) Procedure flowchart. The procedure was implemented following the flowchart step by step, where it began at “START” and finished at “COMPLETE”. ATP, adenosine-5'-triphosphate; CSD, clinically significant drift; FFR, fractional flow reserve; MEMS-PMC, MEMS-sensor based pressure microcatheter; P_a , aortic pressure; P_d , coronary distal pressure; PW, pressure wire

in Figure 2b. As illustrated briefly, when physiology assessment is necessary, the FFR values of each interrogated vessel were first measured by the MEMS-PMC over a PW (PressureWire Certus, Abbott Vascular, St. Paul, MN, USA), and then the PW alone (Figure 2b). Since such a design requires the lesion being interrogated by both the MEMS-PMC and the PW, anticoagulation was proactively administered the same as in standard PCI procedures (100 U/kg unfractionated heparin). Meanwhile, an activated clotting time > 250 s was constantly monitored in procedure. Guiding catheters of 6Fr or larger were used

in procedures. Both MEMS-PMC and PW were calibrated (“zeroed”) at patient’s heart level with heparinized saline immersion. After entry, the PW first equalized its sensor at coronary ostium and was then advanced until its sensor reached 2–3 cm distal to the lesion, where a stable distal-to-aortic pressure ratio (P_d/P_a) at resting was recorded by the operator. The MEMS-PMC was equalized at the same anatomic position after calibration. Navigated by the distal marker band, the MEMS-PMC was advanced ~2 mm proximal to PW’s sensor. The stable resting P_d/P_a ratios of both systems were recorded by the

operator. Before inducing hyperemia, 100–200 μg intracoronary nitroglycerin was administered via guiding catheter to relieve possible vasoconstriction. For maximum vasodilation, ATP (20 mg per 2 ml ampule, 1:10 diluted before use) was chosen for its established pharmacological equivalence with adenosine.¹⁹ Intravenous ATP infusion via antecubital vein was performed with flow rate based on $140 \mu\text{g ATP}\cdot\text{kg}^{-1}\cdot\text{min}^{-1}$ by patient's weight. About 2 min post-infusion, when the MEMS-PMC P_d/P_a declined to the minimum and its waveform plateaued for at least five consecutive cardiac cycles, the stable P_d/P_a of MEMS-PMC at nadir was recorded as its FFR (Figure 2c). Then, the MEMS-PMC was pulled back to equalization position for checking drift. If the MEMS-PMC's P_d/P_a failed to be within 0.97–1.03 at the check position, it was re-equalized in situ. After re-equalization, the MEMS-PMC's FFR measurement would be repeated. Otherwise it would be completely withdrawn out of the body, and the PW FFR measurement was started immediately.

The waveforms of MEMS-PMC and PW were closely monitored throughout the procedure, and saline flush or guiding catheter adjustment was applied if any pressure damping was suspected. An on-site clinical research coordinator aided all procedural steps, and the coordinator's records were reviewed weekly by an independent clinical research associate.

2.4 | Data collection, management, and analysis

Raw data collected on-site were approved by the Medical Research and Biometrics Center (MRBC) affiliated with the National Center for Cardiovascular Diseases, China. Once collected, the raw data were logged and managed in MRBC's independent Electronic Data Capture (EDC) system. Upon completion of the enrollment phase, the MRBC locked the EDC system to prevent any further modification. The MRBC also remained blinded to the FFR data until the cohort for full analysis was determined, then, it subdivided the per-protocol group from the full analysis cohort and performed all required statistical analyses (Figure 2a).

2.5 | Quantitative coronary angiography

Two-dimensional quantitative coronary angiography (2D-QCA) analysis was performed by an independent core laboratory (Core Medical, Beijing, China) using Medis QAngio XA (version 7.3, Medis medical imaging system, Leiden, the Netherlands). In the QCA, the RVD and DS% of the target lesion were specifically analyzed.

2.6 | Primary and secondary endpoints

The primary endpoint for this study is the mean bias between FFR of MEMS-PMC and PW, as assessed by Bland–Altman analysis. Secondary endpoints include the Pearson correlation coefficient (r), vessel –/patient-level diagnostic performance, the independent predictors for diagnostic agreement, Passing–Bablok regression, ROC analysis, device success and drift.

Using PW FFR ≤ 0.80 as the dichotomous threshold for physiological significance, the MEMS-PMC's diagnostic performance is presented in standard proportions with 95% confidence interval (CI) evaluated by the Clopper–Pearson method. Clearly, at vessel level the diagnostic result of MEMS-PMC is either agreed or disagreed with that of PW. For patients with FFR measured in more than one vessel, their patient-level diagnostic results were defined by the following:

Patient – level diagnostic result

$$= \begin{cases} \text{Agreed, if the two systems agreed in all vessels;} \\ \text{Disagreed, if the two systems disagreed in at least one vessel.} \end{cases}$$

To analyze the independent predictors for the binary results of diagnostic agreement, logistic regression was used. For other independent predictors, multiple linear regression was used. ROC curve analysis for MEMS-PMC was performed to obtain optimal cutoff as well as to determine the area under the curve (AUC). The drift magnitude is the absolute arithmetic difference between P_d/P_a at check position and 1.00. The mean drift magnitude of both systems was compared using the Wilcoxon rank-sum test. The device success is defined when the system acquires clinically acceptable FFR (with the magnitude of drift ≤ 0.03). The success rates of the two systems were compared using Fisher's exact test. The clinically significant drifts (CSD) are drifts with magnitude > 0.03 (Figure 2c) and were recorded at each occurrence. The CSD rate of both systems was compared using chi-square test. SAS (version 9.4, SAS Institute, Cary, USA) and MedCalc (version 19.1, MedCalc Software, Ostend, Belgium) were used for all statistical analyses and figure plots. Variables are presented in mean \pm SD, and statistical significance is regarded at p -value < 0.05 .

2.7 | Sample size calculation

The sample size was derived from the postulated mean bias between MEMS-PMC and PW. The null hypothesis (H_0) and the alternative hypothesis (H_1) were:

$$H_0 : |FFR_{PMC} - FFR_{PW}| > \delta$$

$$H_1 : |FFR_{PMC} - FFR_{PW}| \leq \delta$$

where $|FFR_{PMC} - FFR_{PW}|$ represents the mean absolute difference (bias) between MEMS-PMC FFR and PW FFR, δ is the non-inferiority margin, for example, $\delta = 0.03$ at FFR = 0.8.¹⁴ The Bland–Altman mean bias of optical-sensor PMC was reported as -0.022 with a SD of 0.049,¹⁴ thus the mean bias between MEMS-PMC and PW was presumed to be -0.022 with a SD of 0.05. The MEMS-PMC was considered non-inferior to PW only if the difference in FFR between the two systems was ≤ 0.03 ($\delta = 0.03$). Setting the two-sided level of significance to 0.05, to reach 95% statistical power a minimum of 207 patients must be enrolled. Considering potential 10–15% loss in patient selection,²⁰ a total of 239 patients were required for the study.

2.8 | Data extraction of published studies

For further comparative analysis, FFR data were extracted from previously published figures²¹ using methods similar to other groups.^{22,23} Specifically, X and Y coordinates of dots in the Bland–Altman plot were retrieved using semiautomatic plot-digitizing software (Version 4.2, WebPlotDigitizer, San Francisco, CA, USA). The paired FFR values, measured simultaneously from two piezoresistive PWs, were resolved from these X and Y values. To ensure the precision of extracted data, the paired FFR values were re-plotted using Bland–Altman analysis (MedCalc Software, Ostend, Belgium) and its mean bias with 95% limits of agreement (LoA) were compared with the

TABLE 1 Baseline characteristics of per-protocol cohort

Patients (n = 224)		
Age (year, mean ± SD)		60 ± 9
Male (%)		143 (63.8%)
Body mass index, kg/m ² (mean ± SD)		25.0 ± 3.3
Tobacco use (%)		58 (25.9%)
Hypertension (%)		141 (62.9%)
Diabetes mellitus (%)		62 (27.7%)
Prior myocardial infarction (%)		13 (6.3%)
Classification of NYHA heart function		
I		173
II		49
III		2
Vessels (n = 229)		
Vessels interrogated		
LAD		155 (67.7%)
LCX		19 (8.3%)
RCA		52 (22.7%)
Others		3 (1.3%)
Lesions		
Location		
Proximal		88 (38.4%)
Mid		129 (56.3%)
Distal		12 (5.3%)
Length (mm) (QCA)	Mean ± SD	15.7 ± 8.8
Specific types		
Diffuse (>20 mm)		55 (24.0%)
Bifurcated		54 (23.6%)
DS (%) (QCA)	Mean ± SD	49 ± 11
	≤50	101 (44.1%)
	>50	128 (55.9%)
RVD (mm) (QCA)	Mean ± SD	3.0 ± 0.5

Note: The baseline characteristics of the patients, their vessels and lesions are listed in the table, where “Vessels interrogated – Others” include: one diagonal branch, one obtuse marginal artery and one posterior descending artery. Angiographic lesion characteristics concluded by QCA are specified, where diffuse lesions are the lesions longer than 20 mm. Abbreviations: DS, diameter stenosis; LAD, left anterior descending artery; LCX, left circumflex artery; NYHA, New York Heart Association; QCA, quantitative coronary angiography; RCA, right coronary artery; RVD, reference vessel diameter.

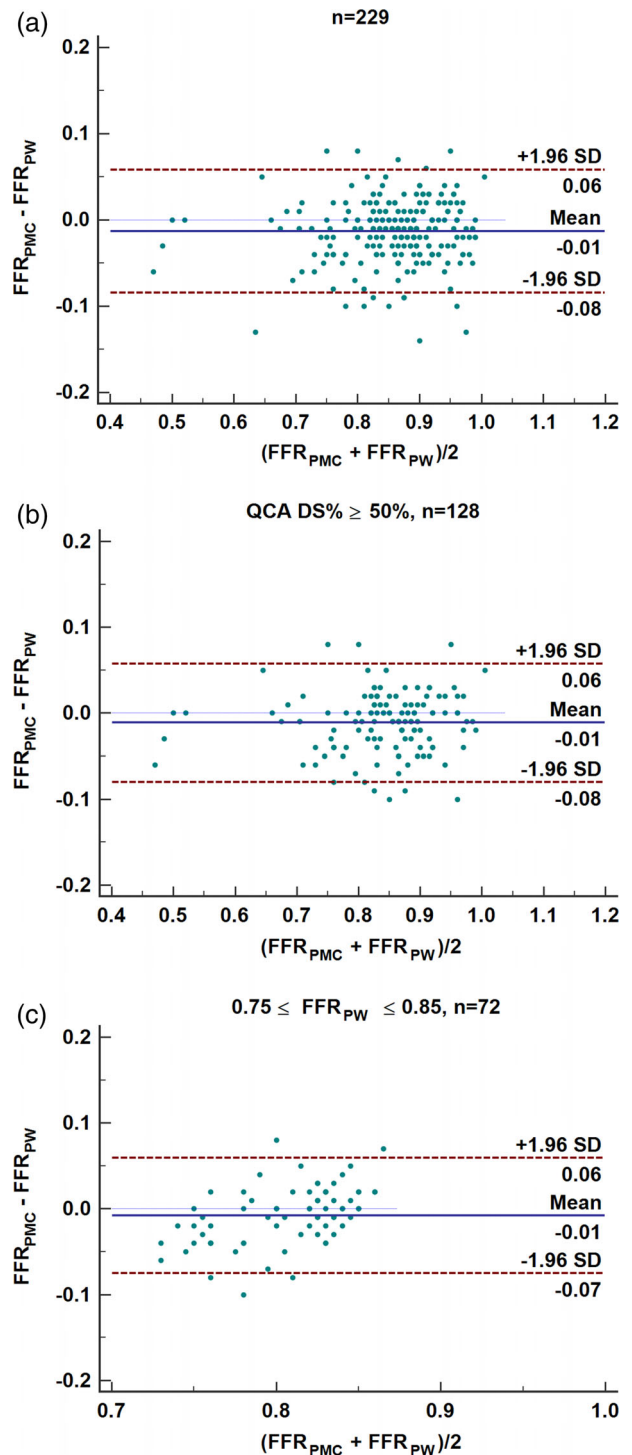


FIGURE 3 Per-protocol cohort and subgroup Bland–Altman analysis results for FFR_{PMC} and FFR_{PW} values. (a) The Bland–Altman mean bias and 95% LoA of FFR_{PMC} and FFR_{PW} in all vessels (n = 229); (b) Bland–Altman plot of FFR_{PMC} and FFR_{PW} in vessels with DS ≥ 50% (n = 128), in which the corresponding mean bias and 95% LoA are concluded; (c) Bland–Altman plot of FFR_{PMC} and FFR_{PW} in vessels with 0.75 ≤ FFR_{PW} ≤ 0.85 (n = 72), in which the corresponding mean bias and 95% LoA are concluded. DS, diameter stenosis; FFR_{PMC}, MEMS-PMC FFR; FFR_{PW}, PW FFR; LoA, limits of agreement

originally published values. Two investigators (C.L. and L.S.) independently performed this process and results were cross-reviewed.

3 | RESULTS

3.1 | Enrollment and baseline characteristics

From May 2018 to February 2019, a total of 242 patients were enrolled in four participating centers, and 239 of them had FFR measured by both systems. Of these 239 patients, 224 had measurements finished per clinical protocol (Figure 2a). In five patients, FFR was measured in more than one vessel, thus resulting 229 vessels with valid FFR measurements. The final statistical power based on 224 patients is 95.9%, which exceeds 95% in the original design. The left anterior descending artery was the most

interrogated vessel, and the most assessed lesion is in the middle of the arteries (56.3%) (Table 1). QCA analysis of 229 interrogated vessels shows that all lesions have an average DS of $49 \pm 11\%$ with 55.9% vessels of DS > 50%, 17.9% has diameter < 2.5 mm, and the mean RVD is 3.0 mm (Table 1). Online supplementary eFigure 2 shows the histogram for RVD and DS distributions.

3.2 | Primary endpoints

3.2.1 | Overall and subgroup Bland–Altman analysis

Bland–Altman analysis shows that the MEMS-PMC has a mean bias of -0.01 ($p < .0001$, 95% Confidence Interval [CI]: -0.018 to -0.008)

TABLE 2 Performance summary of MEMS-PMC

MEMS-PMC diagnostic performance at vessel-level and patient-level.					
		Vessel-level (n = 229)	Patient-level (n = 224)		
Accuracy [95%CI]		93.4% [89.4–96.3%]	93.3% [89.2–96.2%]		
Sensitivity [95%CI]		91.3% [79.2–97.6%]	91.3% [79.2–97.6%]		
Specificity [95%CI]		94.0% [89.5–97.0%]	93.8% [89.2–96.9%]		
+LR [95% CI]		15.19 [8.51–27.13]	14.77 [8.28–26.37]		
–LR [95% CI]		0.09 [0.04–0.24]	0.09 [0.04–0.24]		
Disease prevalence		20.09% [15.10–25.87%]	20.54% [15.44–26.42%]		
MEMS-PMC subgroup diagnostic performance: RVD < 2.5 and \geq 2.5 mm.					
		RVD < 2.5 mm (n = 41)	RVD \geq 2.5 mm (n = 188)	p-value	
Bland–Altman	Mean bias	–0.02	–0.01	–	
	95% LoA	[–0.09, 0.05]	[–0.08, 0.06]	–	
Accuracy [95%CI]		90.2% [76.9–97.3%]	94.2% [89.8–97.0%]	.317 (Fisher's exact)	
Comparison of device success rates between MEMS-PMC and PW systems					
		MEMS-PMC	PW	p-value	
Device success rate % (fraction)		97.5% (238/244)	96.3% (235/244)	.430 (McNemar)	
Comparison of drifts between MEMS-PMC and PW systems					
		MEMS-PMC	PW	p-value	
Total times of drift check		263	282	–	
CSD rate % (fraction)		9.5% (25/263)	16.7% (47/282)	.014 (chi-square)	
Drift magnitude (mean \pm SD)		0.021 \pm 0.031	0.024 \pm 0.033	.263 (Wilcoxon rank sum)	
Comparison of mean FFR values between MEMS-PMC and PW					
		MEMS-PMC	PW	p-value	
FFR (mean \pm SD)		0.85 \pm 0.09	0.86 \pm 0.09	<.0001 (Wilcoxon rank sum)	

Note: Using $FFR_{PW} \leq 0.80$ as cutoff, the accuracy, sensitivity, specificity, positive and negative likelihood ratio of the MEMS-PMC at vessel level and patient level, with respective 95% CIs, are listed. Size of each level and the statistical method are specified. The Bland–Altman mean bias and 95% LoA at subgroups: RVD < 2.5 mm and RVD \geq 2.5 mm, are listed. Using PW $FFR \leq 0.80$ as cutoff, the accuracies of these two subgroups are compared. Size of each subgroup and the statistical method are specified. Device success, defined as successful FFR measurement with drift magnitude ≤ 0.03 , between the two systems are compared, with statistical method specified; the number of total drift checks, CSD rate, and drift magnitude (mean \pm SD) between the two systems are compared, with statistical method and p-values specified. Drift magnitude is the absolute arithmetic difference between the P_d/P_a at check position and 1.00, p is the statistical significance level.

Abbreviations: +LR, positive likelihood ratio; –LR, negative likelihood ratio; CI, confidence interval; CSD, clinically significant drift; FFR, fractional flow reserve; LoA, limits of agreement; RVD, reference vessel diameter.

compared with PW, with 95% LoA $[-0.08, 0.06]$ (Figure 3a). Such bias and LoA are essentially unchanged when different subgroups are selected, for example, the subgroup with DS $\geq 50\%$ ($n = 128$, Figure 3b), the subgroup with PW FFR between 0.75 and 0.85 ($n = 72$, Figure 3c), or the subgroup with RVD > 2.5 mm ($n = 188$, Table 2). For RVD < 2.5 mm, Bland-Altman bias of MEMS-PMC is -0.02 (95% CI: -0.0341 to -0.0111) with a 95% LoA $[-0.09, 0.05]$ (Table 2).

3.3 | Secondary endpoints

3.3.1 | Correlation, regression, diagnostic performance, and ROC analysis

Pearson analysis shows strong correlation between MEMS-PMC and PW ($r = 0.9214$, $p < .0001$, [95% CI: 0.8963 to 0.9373], Figure 4a). The Passing-Bablok regression line has an intercept at -0.01 ($p < .0001$, 95% CI: -0.08 to -0.01) and a slope of 1.00 (95% CI: 1.00–1.08, Figure 4b), demonstrating high interchangeability between the two systems. Using the dichotomous threshold PW FFR ≤ 0.80 for physiological significance, MEMS-PMC achieved high vessel-level diagnostic accuracy (93.4%, [95% CI: 89.4–96.3%]). The vessel- and patient-level diagnostic accuracy, sensitivity, specificity, positive and negative likelihood ratios of MEMS-PMC are summarized in Table 2. In addition, the diagnostic accuracy of MEMS-PMC remains statistically on the same level whether RVD is < 2.5 or ≥ 2.5 mm ($p = .317$, Table 2).

If considering the FFR “gray zone” (0.75–0.80) and defining concordance as the FFR of PW and MEMS-PMC are both ≥ 0.75 , or both ≤ 0.80 , MEMS-PMC’s concordance is 99.6% (95% CI: 97.6–99.9%).

Using the same PW FFR ≤ 0.80 threshold, the MEMS-PMC ROC curve analysis has an AUC of 0.979 ($p < .0001$, [95% CI: 0.950 to 0.993]) and the optimal cutoff is at 0.80 (online supplementary eFigure 3). Further analysis shows that if PW FFR < 0.75 , instead of ≤ 0.80 , is regarded as physiologically significant,¹ the ROC analysis indicates 0.72 as MEMS-PMC’s new optimal cutoff (online supplementary eFigure 4). Using MEMS-PMC FFR ≤ 0.72 , 97.8% of the lesions’ classification by MEMS-PMC would agree with those classified by PW FFR < 0.75 (online supplementary eFigure 4).

3.3.2 | Multivariate analysis

Logistic regression for binary diagnostic agreement results (“agreed” or “disagreed”) shows: (a) if the FFR bias between the two systems is excluded, the MEMS-PMC FFR is the only significant independent predictor ($p = .039$); (b) if the FFR bias between the two systems is introduced, the absolute bias becomes the only independent predictor ($p < .001$). Multiple regression analysis shows: (a) for absolute FFR bias, RVD and diffuse lesion are significant independent predictors; (b) for FFR bias with signs (+ or -), RVD, smoking, and distal lesion are

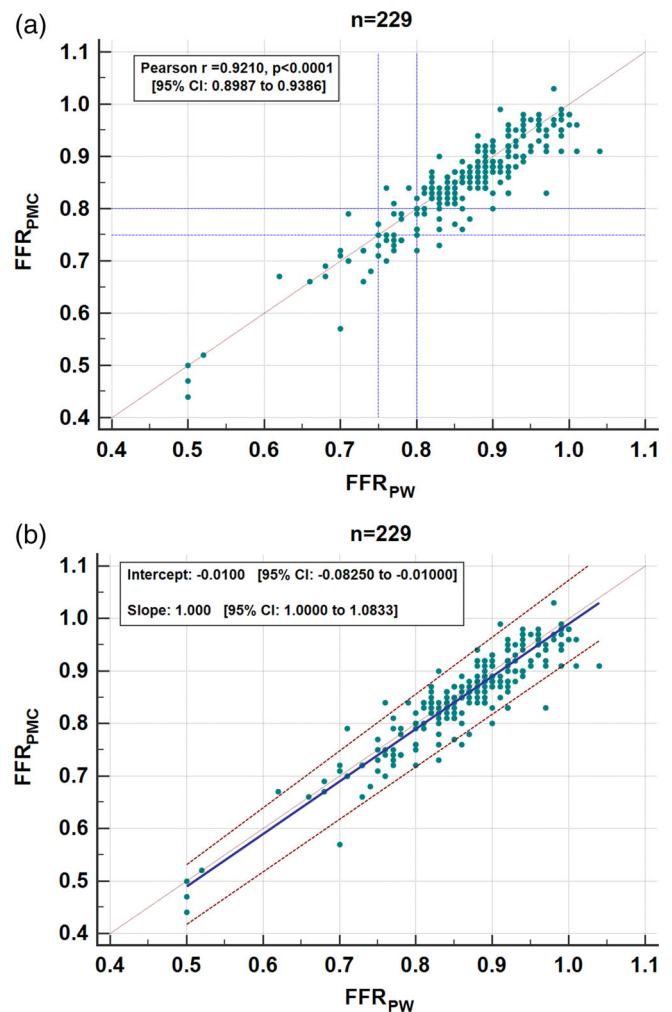


FIGURE 4 Pearson correlation and Passing-Bablok regression analyses of FFR_{PMC} and FFR_{PW} ($n = 229$). The correlation analysis concludes a coefficient of 0.921 with 95% CI. The regression analysis concludes a 1.0 slope and a -0.01 intercept of regression line for FFR_{PMC} and FFR_{PW} , with their respective 95% CIs. CI, confidence interval; FFR_{PMC} , MEMS-PMC FFR; FFR_{PW} , PW FFR

significant independent predictors. The lists of variables included in Logistic regression and multivariate regression analyses are presented in online supplementary eTables 4 and 5.

3.3.3 | Device success and evaluation of drift

No significant difference in success rate was found between MEMS-PMC and PW (MEMS-PMC: 97.5%, PW: 96.3%, $p = .43$, Table 2). In total, there were more drift checks in PW compared to MEMS-PMC when all 239 patients were considered (Table 2). The mean drifts of MEMS-PMC and PW are similar (MEMS-PMC: 0.021, PW: 0.024, $p = .263$, Table 2), but the PW CSD rate is nearly twice that of MEMS-PMC (MEMS-PMC: 9.5%, PW: 16.7%, $p = .014$, Table 2).

4 | DISCUSSION

This is the first clinical study investigating the newly developed piezoresistive pressure microcatheter system for FFR measurement, using a conventional pressure wire system as the reference standard. To date, the trial reported here is also the largest study (with per-protocol data of 224 patients) evaluating any type of microcatheter-based FFR measurement systems in comparison with the conventional pressure wire system. In this multicenter, prospective clinical study, the new piezoresistive-MEMS-sensor PMC system exhibited excellent measurement agreement and diagnostic performance. For example, our Bland–Altman analysis shows the mean bias between the two systems is as small as -0.01 ; in addition, the Bland–Altman 95% LoA [$-0.08, 0.06$] are similar to those of paired conventional PWs found in the COMET study: [$-0.06, 0.06$].²¹ Passing-Bablok regression analysis shows MEMS-PMC having a constant difference -0.01 . With respect to the diagnostic agreement, using the dichotomous cutoff $PW \leq 0.80$ as reference, the MEMS-PMC has accuracy, sensitivity, and specificity of 93.4, 91.3, and 94.0%, respectively; when FFR “gray zone” (0.75–0.80) is considered, 99.6% (95% CI: 97.6–99.9%) of the paired MEMS-PMC and PW measurements are concordant (both ≥ 0.75 or both ≤ 0.80 in the same vessel). These results imply MEMS-PMC is highly effective for accurately measuring FFR in the cathlab.

Different subgroup accuracies of MEMS-PMC FFR are: 96.6% (when its own FFR < 0.75), 100% (when its own FFR > 0.85), 81.3% (when its own FFR 0.75–0.85). The lowest is when its own FFR is between 0.75 and 0.85. This result is consistent with other studies, for example, Wakasa et al. reported that 18.7% of the 235 lesions with FFR 0.77–0.82 would be reclassified as a result of pressure drift.²⁴ To explain such “notched” accuracy distribution, the theory of probability strongly reasons that the closer the true physiological value is to the dichotomous threshold 0.80, the measured value would more likely fall on either side of threshold with a probability of up to 50%.²⁵ This phenomenon was indeed observed in previous clinical studies. For example, in the COMET trial, even for FFR values simultaneously measured from paired conventional PWs in the same vessel,²¹ the PW’s accuracy is $< 85\%$ upon its own FFR 0.75–0.85, when taking the other PW as reference with ≤ 0.80 as cutoff. The pioneering landmark studies confirmed there is a certain range of FFR spectrum without a clear “either-or” physiological implication,^{1,2} and the “notched” accuracy distribution reports a reiteration of such fact. It reminds and encourages that we clinicians should always fetch broadened and more comprehensive information beyond a single number when making a clinical decision.^{25–27}

In the literature, a hypothesis exists that the fiber-optic based pressure sensor has less drift compared with piezoresistive sensors.¹² However, until now, this hypothesis has not been well verified: while Menon et al. found optical-sensor PMC has smaller mean drift than piezoresistive PW ($p = .014$),²⁸ Wijntjens et al.,¹³ Fearon et al.,¹⁴ and Ali et al.¹⁵ all reported that the mean drift of the two systems do not differ statistically ($p = .07, .66, \text{ and } .38$, respectively). The findings are similar when comparing the mean drift of optical-sensor PW with piezoresistive PW.²¹ As of the drift with clinical significance, Menon

et al. reported a numerically lower drift occurrence rate for PMC without p -value (PMC: 13%; PW: 33%), while Wijntjens et al.¹³ and Fearon et al.¹⁴ showed the difference was not statistically significant ($p = .76$ and $.10$, respectively). Recently, Beygui et al. found the optical-sensor based PMC has a statistically lower mean drift than the optical-sensor based PW,²⁹ implying the PW seems more vulnerable to drift.²⁹ In our study, we found that MEMS-PMC has: (a) similar mean drift as the PW ($p = .263$, Table 2), and (b) statistically less clinically significant drift (CSD) rate than the PW ($p = .014$, Table 2). One reason for PW’s higher CSD rate may be due to the dis- and re-connection of the PW electrical end during procedures, which is not uncommon in daily clinical practice while using PW. However, determining the exact reason(s) is beyond the scope of this clinical study.

In this study, MEMS-PMC has the same device success rate as PW (97.5 vs. 96.3%, $p = .43$), and all MEMS-PMCs successfully crossed the lesions. The success results of optical-sensor PMC are similar: 97% (94/97, CONTRACT),³⁰ 97% (237/245, ACIST-FFR),¹⁴ 97% (972/1000, pre-PCI, FFR-SEARCH)¹¹ and 94% (31/33, FFR-DS).²⁹ During the study, no thrombus was observed on the devices in any of the enrolled 242 patients, nor was there any other serious adverse event. Thus, the MEMS-PMC is safe to use for routine clinical FFR measurement. Combined with historical safety data from other researchers: Diletti et al. (15 patients),¹² Menon et al. (50 patients),²⁸ Fearon et al. (169 patients)¹⁴ and van Bommel et al. (959 patients),¹¹ this study has reconfirmed the safety of PMC systems for clinical use.

4.1 | Limitation of the study

In this study, the MEMS-PMC FFR was measured over a PW rather than a conventional guidewire, and the measurement of FFR was not randomized. This is regarded as reasonable because FFR is already proven to be highly reproducible between repeated measurements,³¹ and we believe that randomizing the measurements between the two systems would not change our results. As adopted in this study, using a pressure wire to guide the MEMS-PMC saved time and reduced radiation exposure; if MEMS-PMC FFR was to be measured over a conventional guidewire, the lesions would be crossed by both a conventional guidewire and a pressure wire, adding the risk of complications. Further, using a PW as a conventional guidewire for PMC FFR measurement was commonly adopted in other published studies. Our study did not follow up FFR-measured patients for any outcomes, since such prognostic relation has already been established.³² Intra-vascular imaging, if routinely being performed as part of the procedure, may provide more anatomic information about vessels in which FFR of the MEMS-PMC and PW disagreed.

5 | CONCLUSION

A new FFR-measuring system featuring MEMS sensor-based PMC compatible with any 0.014” guidewire was evaluated by a multicenter clinical study. This MEMS-PMC has shown a mean bias similar

to the resolution of current PW FFR (-0.01) systems. The MEMS-PMC's agreement with the PW suggests its equivalence in FFR measurement. Combined with its rapid-exchange feature and lower CSD frequency, the MEMS-PMC may become an attractive tool for interventional cardiologists to use for routine physiology assessment.

ACKNOWLEDGEMENTS

We would like to thank the participating patients from all four recruiting centers, and the associated staff for their contributions to this research.

CONFLICT OF INTEREST

William Kongto Hau receives consulting-speaker honoraria from Philips Volcano, Boston Scientific, Abbott Vascular, Vivo-light, and Keya Medical; Allen JeremiasJ. receives unrestricted education grants from and serves as a consultant for Philips Volcano and Abbott Vascular, and he is also a consultant to ACIST Medical and Boston Scientific; Junbo Ge receives a research grant from SINO Medical.

DATA AVAILABILITY STATEMENT

Data subject to third party restrictions The data that support the findings of this study are available from Medical Research & Biometrics Center, National Center for Cardiovascular Diseases, China. Restrictions apply to the availability of these data, which were used under license for this study. Data are available at <http://39.96.78.40/ffricaEDC/> with the permission of the Human Genetic Resources Management Office, Ministry of Science and Technology, China.

ORCID

Chenguang Li  <https://orcid.org/0000-0002-5287-5269>

Junbo Ge  <https://orcid.org/0000-0002-9360-7332>

REFERENCES

1. Bech GJW, De Bruyne B, Pijls NHJ, et al. Fractional flow reserve to determine the appropriateness of angioplasty in moderate coronary stenosis. *Circulation*. 2001;103(24):2928-2934.
2. Tonino PAL, De Bruyne B, Pijls NHJ, et al. Fractional flow reserve versus angiography for guiding percutaneous coronary intervention. *N Engl J Med*. 2009;360(3):213-224.
3. Koolen JJ, Bech GJW, Boersma E, et al. Fractional flow reserve to determine the appropriateness of angioplasty in moderate coronary stenosis. *Circulation*. 2012;103(24):2928-2934.
4. Zimmermann FM, Ferrara A, Johnson NP, et al. Deferral vs. performance of percutaneous coronary intervention of functionally non-significant coronary stenosis: 15-year follow-up of the DEFER trial. *Eur Heart J*. 2015;36(45):3182-3188.
5. Van Nunen LX, Zimmermann FM, Tonino PAL, et al. Fractional flow reserve versus angiography for guidance of PCI in patients with multivessel coronary artery disease (FAME): 5-year follow-up of a randomised controlled trial. *Lancet*. 2015;386(10006):1853-1860.
6. Xaplanteris P, Fournier S, Pijls NHJ, et al. Five-year outcomes with PCI guided by fractional flow reserve. *N Engl J Med*. 2018;379(3):250-259.
7. Patel MR, Calhoun JH, Dehmer GJ, et al. ACC/AATS/AHA/ASE/ASNC/SCAI/SCCT/STS 2017 appropriate use criteria for coronary revascularization in patients with stable ischemic heart disease. *J Thorac Cardiovasc Surg*. 2019;157(3):e131-e161.
8. Sousa-Uva M, Neumann FJ, Ahlsson A, et al. 2018 ESC/EACTS Guidelines on myocardial revascularization. *Eur J Cardio Thorac Surg*. 2019;55(1):4-90.
9. Warisawa T, Cook CM, Akashi YJ, Davies JE. Past, present and future of coronary physiology. *Rev Esp Cardiol*. 2018;71(8):656-667.
10. Jeremias A, Davies JE, Maehara A, et al. Blinded physiological assessment of residual ischemia after successful angiographic percutaneous coronary intervention: the DEFINE PCI study. *JACC Cardiovasc Interv*. 2019;12(20):1991-2001.
11. van Bommel RJ, Masdjedi K, Diletti R, et al. Routine fractional flow reserve measurement after percutaneous coronary intervention. *Circ Cardiovasc Interv*. 2019;12(5):1-9.
12. Diletti R, Van Mieghem NM, Valgimigli M, et al. Rapid exchange ultrathin microcatheter using fibre-optic sensing technology for measurement of intracoronary fractional flow reserve. *EuroIntervention*. 2015;11(4):428-432.
13. Wijntjens GWM, Van De Hoef TP, Kraak RP, et al. The IMPACT study (influence of sensor-equipped microcatheters on coronary hemodynamics and the accuracy of physiological indices of functional stenosis severity). *Circ Cardiovasc Interv*. 2016;9(12):1-8.
14. Fearon WF, Chambers JW, Seto AH, et al. ACIST-FFR study (assessment of catheter-based interrogation and standard techniques for fractional flow reserve measurement). *Circ Cardiovasc Interv*. 2017;10(12):e005905.
15. Ali ZA, Parviz Y, Brinkman M, et al. Pressure wire compared to microcatheter sensing for coronary fractional flow reserve: the PERFORM study. *EuroIntervention*. 2018;14(4):e459-e466.
16. Pouillot C, Fournier S, Glasenapp J, et al. Pressure wire versus microcatheter for FFR measurement: a head-to-head comparison. *EuroIntervention*. 2018;13(15):e1850-e1856.
17. Vranckx P, Cutlip DE, McFadden EP, Kern MJ, Mehran R, Muller O. Coronary pressure-derived fractional flow reserve measurements: recommendations for standardization, recording, and reporting as a core laboratory technique. Proposals for integration in clinical trials. *Circ Cardiovasc Interv*. 2012;5(2):312-317.
18. Pijls NHJ, Kern MJ, Yock PG, De Bruyne B. Practice and potential pitfalls of coronary pressure measurement. *Catheter Cardiovasc Interv*. 2000;49(1):1-16.
19. De Bruyne B, Pijls NHJ, Barbato E, et al. Intracoronary and intravenous adenosine 5'-triphosphate, adenosine, papaverine, and contrast medium to assess fractional flow reserve in humans. *Circulation*. 2003;107(14):1877-1883.
20. Xu B, Tu S, Qiao S, et al. Diagnostic accuracy of angiography-based quantitative flow ratio measurements for online assessment of coronary stenosis. *J Am Coll Cardiol*. 2017;70(25):3077-3087.
21. Stables RH, Elguindy M, Kemp I, et al. A randomised controlled trial to compare two coronary pressure wires using simultaneous measurements in human coronary arteries: the COMET trial. *EuroIntervention*. 2019;14(15):e1578-e1584.
22. Seligman H, Shun-Shin MJ, Vasireddy A, et al. Fractional flow reserve derived from microcatheters versus standard pressure wires: a stenosis-level meta-analysis. *Open Heart*. 2019;6(1):e000971.
23. Demir OM, Mitomo S, Mangieri A, et al. Diagnostic accuracy of microcatheter derived fractional flow reserve. *Am J Cardiol*. 2019;124(2):183-189.
24. Wakasa N, Kuramochi T, Mihashi N, et al. Impact of pressure signal drift on fractional flow reserve-based decision-making for patients with intermediate coronary artery stenosis. *Circ J*. 2016;80(8):1812-1819.
25. Pijls NH, De Bruyne B. Fractional flow reserve, coronary pressure wires, and drift. *Circ J*. 2016;80(8):1704-1706.
26. Wijns W, Pyxaras SA. Chasing Numbers. *JACC Cardiovasc Interv*. 2013;6(3):226-227.
27. Petraco R, Sen S, Nijjer S, et al. Fractional flow reserve-guided revascularization. *JACC Cardiovasc Interv*. 2013;6(3):222-225.

28. Menon M, Jaffe W, Watson T, Webster M. Assessment of coronary fractional flow reserve using a monorail pressure catheter: the first-in-human ACCESS-NZ trial. *EuroIntervention*. 2015;11(3):257-263.
29. Beygui F, Lemaître A, Bignon M, et al. A head-to-head comparison of three coronary fractional flow reserve measurement technologies: the fractional flow reserve-device study. *Catheter Cardiovasc Interv*. 2020;95(6):1094-1101.
30. Masdjedi K, Van Mieghem NM, Diletti R, et al. Navvus FFR to reduce CONTRAst, cost and radiaTion (CONTRACT); insights from a single-Centre clinical and economical evaluation with the RXi rapid-exchange FFR device. *Int J Cardiol*. 2017;233:80-84.
31. Johnson NP, Jeremias A, Zimmermann FM, et al. Continuum of vasodilator stress from rest to contrast medium to adenosine hyperemia for fractional flow reserve assessment. *JACC Cardiovasc Interv*. 2016;9(8):757-767.
32. Johnson NP, Tóth GG, Lai D, et al. Prognostic value of fractional flow reserve. *J Am Coll Cardiol*. 2014;64(16):1641-1654.

SUPPORTING INFORMATION

Additional supporting information may be found online in the Supporting Information section at the end of this article.

How to cite this article: Li C, Yang J, Dong S, et al. Multicenter clinical evaluation of a piezoresistive-MEMS-sensor rapid-exchange pressure microcatheter system for fractional flow reserve measurement. *Catheter Cardiovasc Interv*. 2021;98:E243–E253. <https://doi.org/10.1002/ccd.29678>